Journals of Gerontology: MEDICAL SCIENCES
Cite journal as: J Gerontol A Biol Sci Med Sci 2014 November;69(11):1399–1406
doi:10.1093/gerona/glu048

Advance Access publication April 9, 2014

Special Issue: Brain Aging

Graph Theory Analysis of Functional Brain Networks and Mobility Disability in Older Adults

Christina E. Hugenschmidt,[1] Jonathan H. Burdette,[2] Ashley R. Morgan,[2] Jeff D. Williamson,[1] Stephen B. Kritchevsky,[1] and Paul J. Laurienti[2]

[1]Sticht Center on Aging and Department of Internal Medicine, Section on Gerontology and Geriatric Medicine, Wake Forest School of Medicine, Winston-Salem, North Carolina.
[2]Department of Radiology, Wake Forest School of Medicine, Winston-Salem, North Carolina.

Address correspondence to Christina E. Hugenschmidt, PhD, Section on Gerontology and Geriatric Medicine, Wake Forest School of Medicine, Medical Center Boulevard, Winston-Salem, NC 27157. Email: chugensc@wakehealth.edu

Background. The brain's structural integrity is associated with mobility function in older adults. Changes in function may be evident earlier than changes in structure and may be more directly related to mobility. Therefore, we assessed whether functional brain networks varied with mobility function in older adults.

Methods. Short Physical Performance Battery (SPPB) and resting state functional magnetic resonance imaging were collected on 24 young (mean age = 26.4 ± 5.1) and 48 older (mean age = 72.04 ± 5.1) participants. Older participants were divided into three groups by SPPB score: Low SPPB (score = 7–9), Mid SPPB (score = 10), High SPPB (score = 11–12). Graph theory–based methods were used to characterize and compare brain network organization.

Results. Connectivity in the somatomotor cortex distinguished between groups based on SPPB score. The community structure of the somatomotor cortex was significantly less consistent in the Low SPPB group (mean = 0.097 ± 0.05) compared with Young (mean = 0.163 ± 0.09, p = .03) SPPB group. Striking differences were evident in second-order connections between somatomotor cortex and superior temporal gyrus and insula that reached statistical significance. The Low SPPB group (mean = 140.87 ± 109.30) had a significantly higher number of connections than Young (mean = 45.05 ± 33.79, p = .0003) or High (mean = 49.61 ± 35.31, p = .002) SPPB group.

Conclusions. Older adults with poorer mobility function exhibited reduced consistency of somatomotor community structure and a greater number of secondary connections with vestibular and multisensory regions of the brain. Further study is needed to fully interpret these effects, but analysis of functional brain networks adds new insights to the contribution of the brain to mobility.

Key Words: Physical function—Neuroimaging—Brain aging.

Received December 30, 2013; Accepted March 7, 2014

Decision Editor: James Goodwin, PhD

MUCH research on the effects of aging on mobility has focused on muscle strength and cardiovascular fitness. However, considerable variability in mobility function remains after accounting for these factors. Recently, it has been proposed that changes in the brain and nervous system might account for some of this variability (1).

Behavior and neuroimaging evidence points to a role for the cortex in mobility. Epidemiological studies show that gait speed correlates with cognitive function and that low gait speed or gait abnormalities may precede cognitive decline (2,3). Furthermore, increased cognitive demand, particularly in the domain of executive function, slows gait speed (4), suggesting shared brain resources supporting cognition and mobility.

Structural neuroimaging studies suggest that the prefrontal cortex, which is associated with executive function, is important for mobility, along with frontoparietal sensorimotor regions, basal ganglia, and cerebellum (5–9). Lower regional brain volumes, including in frontoparietal, frontal, and sensorimotor regions, are associated with poorer gait speed, gait characteristics, and balance (5–9). Mobility involves coordination of regions across the brain, and damage to the connections between these regions may contribute to declining mobility function. White matter lesions arising from cardiovascular disease are associated with mobility impairment, especially when they are severe and located in frontal lobe (for review see Zheng and colleagues (10)). Importantly, associations between brain changes and mobility are observed in the absence of frank disease, indicating that brain changes are relevant to even healthy-appearing older adults and may occur early on in mobility decline.

The strong links between white matter health and mobility suggest that brain connectivity is important for mobility

function. However, analysis of structural connectivity cannot directly assess how *functional* connections in the brain differ with mobility impairment. Functional network analyses have the potential to identify alterations in brain function prior to the development of irreparable tissue damage.

Graph theory analysis of functional brain imaging data exploits the complexity of brain connections to characterize the overall functional architecture of the brain network. Rather than ascertaining whether individual brain regions are associated with mobility disability, graph theory analysis treats the brain as one integrated network and asks whether the architecture of communication patterns within that network is altered when mobility is impaired. Here, we analyze functional magnetic resonance imaging data using graph theory (11) to assess differences in functional brain connections across participants with high, mid, and low mobility function determined by Short Physical Performance Battery (SPPB) score (12).

Methods

Participants

Participants included 24 young (mean age = 26.4±5.1, 15 women) and 48 older (mean age = 72.04±5.1, 27 women) participants from two pilot studies examining age-related changes in mobility and brain organization. Study 1 contributed 32 older participants and Study 2 contributed 15. Nine young participants were from Study 1 and 15 from Study 2. The same study staff tested all participants. Exclusion criteria included a Mini-Mental State Examination score greater than 3 *SD*s below age and education adjusted mean (13); reported diagnoses or medications consistent with psychiatric or neurological disorders, head injuries or stroke; evidence of alcoholism using either the Alcohol Use Disorders Identification Test (14) or the Michigan Alcohol Screening Test (15); or moderate hearing loss (no more than 50 dB measured with a digital audiometer (Digital Recordings, Halifax, Nova Scotia) or inability to hear verbal commands given from behind, where they could not see the examiner). Participants reporting a diagnosis of depression were included if they received treatment for at least 2 months and scored less than 16 on the Center for Epidemiological Studies Depression Scale (16) or had study physician approval. All participants had corrected vision of 20/40 or better using a modified Snellen visual acuity exam. Table 1 presents participants' demographic characteristics.

Test of Mobility Function

Mobility function was tested using the SPPB (12), a test of lower extremity function with three parts. Standing balance was assessed by having participants stand with feet in side-by-side, semitandem, and tandem positions for 10 seconds each. Gait speed was assessed with a 4-m walk at usual pace without assistive devices. Time to rise from a chair five times was measured. Each of these tests results in both a measure of time and a performance score ranging from 0–4 (0 indicates that the test was not able to be performed and 4 is the best performance). The three scores are summed to generate the final SPPB score (range: 0–12). Older adults were divided into three groups based on SPPB score cutoffs found to predict risk for mobility-related disability (17). The High SPPB (n = 19) group had total SPPB scores of 11–12, the Mid SPPB (n = 17) group scored 10, and the Low SPPB (n = 12) group scores ranged from 7–9.

Magnetic Resonance Imaging Acquisition

All images were acquired on a 1.5T echo speed horizon LX General Electric scanner with twin speed gradients and a neurovascular head coil (GE Medical Systems, Milwaukee, WI). High resolution T1-weighted structural images were acquired and used for normalization. Resting state blood-oxygen-level dependent functional magnetic resonance imaging images were acquired using a whole-brain gradient-echo echoplanar imaging sequence with the following parameters: 28 contiguous slices; slice thickness = 5 mm; in-plane resolution = 3.75 × 3.75 mm, TR = 2.0. After discarding initial images to allow the signal to reach steady state, the timeseries from Study 1 had 150 images and from Study 2 had 188 images. The optimal duration of a resting state scan needed to accurately estimate network characteristics using graph theory is a matter of current

Table 1. Participant Characteristics

	Older			Younger
	Low SPPB (7–9)	Mid SPPB (10)	High SPPB (11,12)	
n	12	17	19	24
Age (years ± *SD*)	73.7±6.8	71.7±4.9	71.4±3.9	26.4±5.1
Women *n* (%)	7 (58.3%)	9 (52.9%)	11 (57.9%)	15 (62.5%)
SPPB Score ± *SD*	8.62±0.65	10±0	11.21±0.42	11.50±0.88
BMI (kg/m^2)	26.3 (22.6–30.5)	26.9 (24.8–28.0)	27.1 (25.0–29.1)	27.6 (24.7–31.0)
Education (years ± *SD*)	15.0±2.9	14.5±1.9	15.3±2.6	16.0±2.4
MMSE	28.0 (26.0–29.0)	29.0 (28.0–30.0)	28.0 (28.0–30.0)	30.0 (29.0–30.0)

Notes: For variables approximating a normal distribution, means ± standard deviation are presented; non-normally distributed variables are presented as median (interquartile range).

BMI = body mass index; MMSE = mini-mental state examination; SPPB = Short Physical Performance Battery.

investigation, but at this time, scan durations of 5–10 minutes are accepted as reliable (18) and scan times as low as 2–3 minutes may be adequate (19).

Calculation of Brain Networks

The brain network was modeled using graph theory methods on a voxel-wise basis (each voxel is a network node). Resting state functional magnetic resonance imaging data were preprocessed using a band-pass filter (0.009–0.08 Hz) to account for physiological noise associated with cardiac, respiratory, and cerebrospinal fluid changes. Data were normalized to Montreal Neurological Institute space using FMRIB's Software Library. A binary adjacency matrix (A_{ij}) was generated for each subject from the normalized, filtered data. The adjacency matrix is an $n \times n$ matrix, where n is the number of brain voxels (~20,000 in this case). The adjacency matrix defines the presence or absence of a connection between any two nodes i and j and is the basis for generating network metrics.

First, the presence of a connection between two nodes was determined by performing a time series regression analysis that included motion parameters as well as mean global, white matter, and cerebrospinal fluid to further correct for physiological noise. This yielded a cross-correlation matrix representing the Pearson's correlation coefficient between every pair of network nodes. Data were dichotomized, creating the final binary matrix A_{ij}, by thresholding the matrix such that the density of connections was comparable across participants. Specifically, the relationship $S = \log(N)/\log(K)$ was maintained across participants, where N = number of network nodes, K = average node degree, and S was set at 2.0, 2.5, and 3.0. Global network statistics are presented for all three thresholds. The analyses with network parameters mapped back to brain space were performed at $S = 2.5$. Networks generated with $S = 2.5$ have a connection density that fits well with the expected density based on the number of nodes in the networks (11).

Network Metrics

A variety of network properties can be derived from the adjacency matrix. The global metrics calculated for each group (Supplementary Figure 1) include total number of nodes in the connected network component, degree, clustering, and path length. The remainder of the analyses focused on somatomotor cortex connectivity.

A community is a group of nodes that are more connected with each other than to nodes in other communities. More colloquially, a community is a group of brain regions that form a neighborhood. *Network modularity* is a measure that identifies communities (20). Determining the optimal modular partition of the network into communities is an NP-hard problem (21), meaning that different runs of modularity algorithms can result in different modular partitions. Therefore, the Qcut algorithm was run 10 times for each subject. The solution with the highest Q value (a metric describing optimal partitioning) was selected as the representative map of community structure for that subject.

The consistency of community structure across participants was evaluated using a statistic called Scaled Inclusivity (SI) (22). SI measures the overlap of modules across participants while penalizing for disjunction (23). The resulting values range between 0 and 1, where a value of 1 represents perfect consistency of that node in modules across all participants and values less than 1 represent disjunction of modules. In practice, values of SI are much lower than 1 because of the large number of nodes in the network. It is recognized that SI values do not have an intuitive meaning, but the values can be readily compared across groups to determine which group exhibited greater consistency. A detailed review of the SI methodology can be found in (23). Once the consistency of the community structure was determined, data were transformed back into brain space to determine the spatial extent of somatomotor communities.

In order to identify how the somatomotor cortex connects to regions beyond the community boundaries, analyses were performed to identify first- and second-order connectivity. First-order connections are nodes directly connected to the somatomotor cortex. Second-order connections are nodes connected to the neighbors of the somatomotor cortex but not directly to somatomotor cortex. Thus, first-order connections are one step away from the somatomotor area and second-order connections are two steps away (Figure 1). This analysis focused on connections with the pre- and postcentral gyri as defined by the Automated Anatomical Labeling Atlas implemented in WFU Pickatlas software (https://www.nitrc.org/frs/?group_id=46&release_id=1958) (24). The bilateral pre- and postcentral gyri, which comprise primary motor and somatosensory cortex, were combined into a single region-of-interest (ROI) and resliced to match the voxel size of the functional magnetic resonance imaging data ($4 \times 4 \times 5$ mm). The number of connections from each voxel in the ROI to all other brain voxels was computed using the connectivity defined in the adjacency matrix. This yielded new images where each brain voxel contained a value representing the number of connections it receives from voxels in the ROI. For the second-order connections the same process was performed to identify the connections coming from any voxel that had a direct connection with the somatomotor ROI. For second-order connections, an edge was not counted if it was traversed in the first-order analysis. In order to statistically compare the number of first- and second-order connections to a brain region, the average number of connections was calculated for the bilateral pre- and postcentral gyri using the ROI described previously, and for an ROI in the superior temporal gyrus (STG) and insula quantified using a $32 \times 32 \times 20$ mm box-shaped ROI centered at $x = 54$, $y = 12$, $z = 2$ and $x = -54$, $y = 12$, $z = 2$ bilaterally.

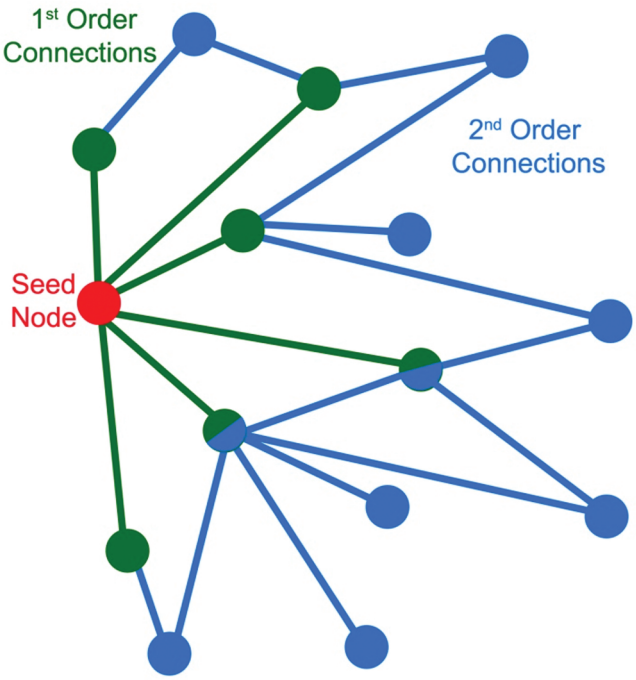

Figure 1. Graphical representation of the concept of first- and second-order connections. The seed node (red) is directly connected to six other nodes (green). Information traverses one edge between the red node and the green nodes. These green nodes each have a first-order connection to the seed. Second-order connections are edges emitting from the direct neighbors of the seed node (blue). Information from the red node must traverse two edges to reach blue nodes. There are a total of 14 second-order connections. Some nodes (green and blue fill) have both first- and second-order connections to the seed node. Note that in this example a single node is serving as the seed. In the analyses described here all nodes within an region-of-interest served as seeds.

Differences in whole-brain and ROI averages of network metrics were statistically compared between the Young and older groups (Low SPPB, Mid SPPB, High SPPB) and between the High SPPB and Low SPPB and Mid SPPB groups with two-tailed *t* tests using SAS version 9.3 implemented in SAS Enterprise Guide 5.1 (SAS Institute Inc., Cary, NC).

Results

Global Network Statistics

Analysis of global network properties included the total number of nodes in the network (*N*), the number of nodes contained in the largest connected component (*Nc*), degree (*K*), path length (*L*), and cluster coefficient (*C*) across all three thresholds evaluated. There were no significant group differences at any threshold. The impact of the various thresholds on network topology was consistent across groups. As expected when increasing the sparsity of a network, more stringent thresholds resulted in a decrease in *Nc*, *K*, and *C*, whereas *L* increased with increasing thresholds (Supplementary Figure 1).

Network Community Structure

Modularity analyses delineate the community structure in complex networks. The overall strength of the community organization for the whole brain was assessed by comparing modularity (*Q*) values. Overall average modularity did not differ between Young and any of the older groups, (Low SPPB: $Q = .677 \pm 0.104$, Mid SPPB: $Q = .728 \pm .068$, High SPPB: $Q = .700 \pm .049$, and Young: $Q = .723 \pm .050$). Modularity analyses were then focused to assess whether community structure of somatomotor cortex differed by mobility function.

Figure 2 shows the consistency of the network communities that encompass the somatomotor cortex for all groups. In these maps, color represents the consistency with which a voxel is included in the somatomotor community across participants. That is, if a voxel is present in the somatomotor community in all participants, it would be 100% consistent across participants. If the spatial location of the somatomotor network is highly variable across participants, consistency would be low. Warm colors show increased consistency and cool colors show more variability across participants.

The community in the region of the somatomotor cortex included bilateral pre- and postcentral gyri as well as medial somatomotor areas. The medial region of the community included primary somatomotor cortex and extended anteriorly into the supplementary motor area. It is visually evident that the somatomotor community is most variable across participants in the Low SPPB group. The average SI value for the somatomotor module was 59.5% higher for the Young group

(mean = 0.163 ± 0.09) than the Low SPPB group (mean = 0.097 ± 0.05, $p = .03$). SI for the Young group was more similar to the Mid (0.156 ± 0.08, $p = .70$) and High (0.143 ± 0.10, $p = .67$) groups. No statistically significant differences were observed between the High SPPB group and the Low ($p = .15$) or Mid ($p = .67$) groups. Qualitatively the communities are in the same regions in all groups; that is, differences between groups were not due to a spatial reorganization of the somatomotor community in the Low SPPB group, but to a reduction in the consistency across participants.

First- and Second-Order Connections

Analysis of community structure yields information about the somatomotor community within the brain network but does not inform us how that community interacts with other brain regions. Therefore, patterns of connectivity between the somatomotor cortex and the rest of the brain were evaluated.

Figure 3 shows regional maps of first-order connectivity for each group. Color represents the average number of connections across participants. Warm colors show the highest number of connections, whereas cool colors reflect lower connectivity. The majority of first-order connections from somatomotor cortex are with itself. This is not surprising given that the community structure analysis identifies highly interconnected nodes. It is visually apparent that first-order connections in older adults with poorer mobility function are fewer, as in the community structure analysis. However, differences in the mean of first-order connections within the somatomotor cortex were not statistically different between Young (mean = 33.50 ± 23.34) and Low SPPB (mean = 26.34 ± 31.28, $p = .36$), Mid SPPB (mean = 40.90 ± 34.76, $p = .42$), or High SPPB (mean = 39.94 ± 41.79, $p = .55$). There was also no significant difference noted between the High SPPB group and the Low ($p = .30$) or Mid ($p = .94$) groups.

Figure 4 shows the regional distribution of second-order connections with the somatomotor cortex. Note that the color scale has changed from Figure 1 to accommodate the increase in the overall number of connections. In High SPPB and Young groups, the regions with the greatest number of connections are still largely within somatomotor cortex. There were no significant differences in the number of second-order connections in the somatomotor area between Young (mean = 48.93 ± 23.72) and Low SPPB (mean = 40.23 ± 22.92, $p = .30$), Mid SPPB (mean = 56.80 ± 40.16, $p = .43$), or High SPPB (mean = 57.28 ± 46.74, $p = .45$) groups. There were

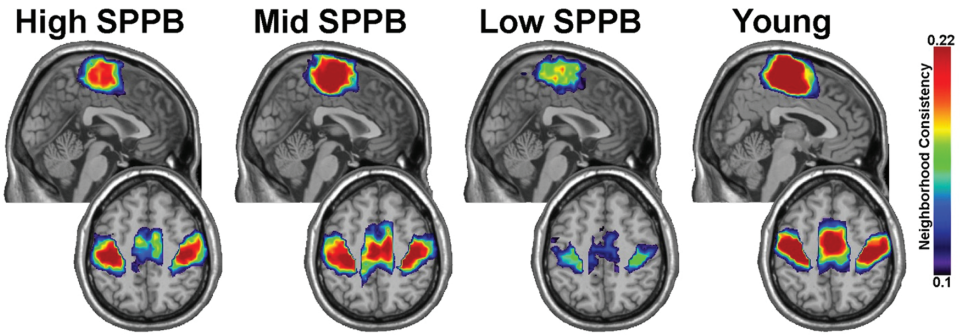

Figure 2. The consistency of the somatomotor community across participants. The community included bilateral and medial sensory and motor cortical areas. A direct comparison of the consistency values across groups shows a reduction in the Low Short Physical Performance Battery group. For each group the upper image is a midsagittal image showing medial somatomotor areas. The lower image for each group is an axial slice showing the lower edge of the medial region and the bilateral somatomotor cortices.

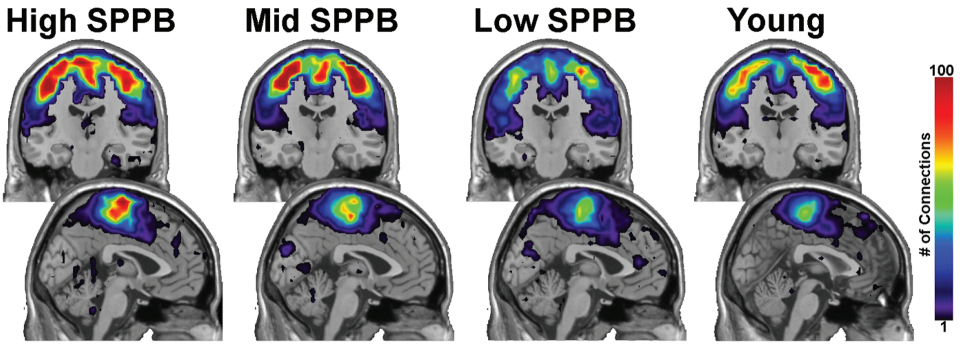

Figure 3. First-order connections from somatomotor cortex. The majority of first-order connections are contained within the somatomotor regions. The images in the upper part of the figure are coronal slices through the somatomotor cortex. The lower images are midsagittal slices. Note that the color bar indicates the average number of connections across all participants in a group.

also no statistically significant differences between the High SPPB group and the Low ($p = .25$) or Mid ($p = .97$) groups.

However, the SPPB groups were clearly distinguished by second-order connectivity from the somatomotor cortex to the STG and insula. The magnitude and spatial extent of second-order connections with STG and insula increased as mobility function decreased (Figure 5A). The connection counts shown in Figure 5B replicated the visually apparent patterns in the brain images. The Low SPPB group had the highest mean number of connections (140.87 ± 109.30) followed by the Mid SPPB group (70.35 ± 51.20). The High SPPB (49.61 ± 35.31) and Young (45.05 ± 33.79) groups had the lowest number of connections. Statistical comparisons showed the Low SPPB group had a significantly greater number of connections than the Young group ($p = .0003$) and the High SPPB group ($p = .002$). A trend for difference was apparent between the Mid SPPB group and Young group ($p = .06$), though not between the Mid and High SPPB ($p = .16$) or Young and High ($p = .67$) groups.

The relationship between SPPB score and second-order connections from somatomotor cortex to the STG and insula was further evaluated using regression analysis (Supplementary Figure 2). The data demonstrated a significant (F [1, 70] = 9.37, $p = .003$) relationship with $R^2 = .12$, meaning approximately 35% of the variance in SPPB score can be accounted for by the number of second-order connections with the STG and insula.

Discussion

We investigated associations between mobility function in older adults measured with the SPPB and the network structure of the brain, particularly connections with the somatomotor module. We observed that the community structure of the somatomotor cortex is more variable in older adults in the Low SPPB group (SPPB < 10) and largely preserved in older adults in the High and Mid SPPB groups. In addition, the groups are clearly differentiated by a pattern of increased second-order connections between somatomotor cortex and a region including the STG and posterior insula. To our knowledge, this is the first time the relationship between mobility function and functional brain networks has been investigated.

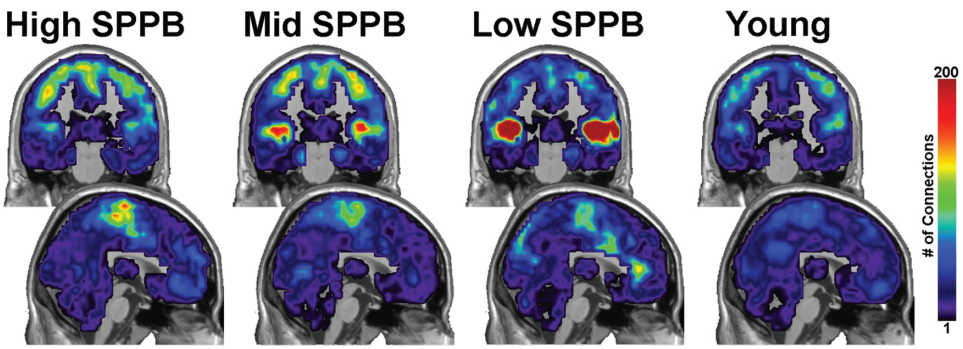

Figure 4. Second-order connections from somatomotor cortex. Second-order connections to the bilateral superior temporal gyrus/posterior insula were significantly increased with decreasing mobility function. The upper images are coronal slices through somatomotor cortex and lower images are midsagittal slices. Note that the scale on the color bar has increased from Figure 3.

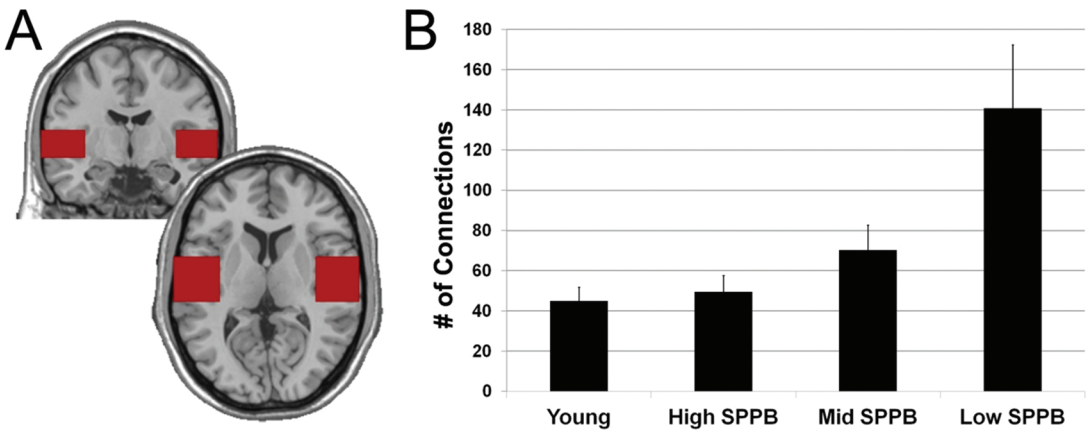

Figure 5. Second-order connections in the superior temporal cortex. (**A**) Depiction of the region-of-interest used to quantify the number of connections from somatomotor cortex to the superior temporal cortex. (**B**) The number of connections in superior temporal cortex averaged across individuals in each group. Error bars indicate the standard error for the group.

The findings of enhanced connectivity with the STG and posterior insula associated with decreased mobility function were unanticipated but consistent with recent observations from a study that used functional near infrared spectroscopy (fNIRS) to evaluate the neural effects of degrading visual and proprioceptive information in healthy young adults during a postural task (25). In that study, Karim and colleagues observed that when visual and proprioceptive information were degraded, blood flow to the posterior insula and STG increased in regions that match our observed regions of increased connectivity in older adults with poor mobility function. They hypothesized that less reliable visual and proprioceptive information resulted in compensatory increases in vestibular contribution to balance.

Mobility requires integration of visual, somatosensory, vestibular, and cognitive information, and these inputs come together in the insula (26). Recent meta-analyses of functional imaging studies of the insula are converging on the idea that the insula has at least three functionally distinct subregions, with the posterior, where we noted increased connectivity, showing links to somatomotor function (27,28). Vestibular processing is highly distributed and does not have a primary cortex in the same way that primary visual or auditory areas exist (26,29). The largest inputs from the vestibular branch of cranial nerve VIII go to multimodal regions of the thalamus and cortex, particularly the insula and STG (26,30). The insula and STG, along with somatomotor cortex, are part of a distributed network receiving vestibular information including projections from primary somatosensory cortex, and primary auditory and auditory association cortices in the STG (27,29). The insula has efferent projections throughout the brain (26), including projections to supplementary motor and secondary somatosensory regions (31). Closer inspection of the maps of second-order connections shows low level connectivity with all of these regions.

Previous studies of brain structure and mobility have found associations with the volume of subcortical brain regions known to be related to movement, such as the basal ganglia and cerebellum (5,7), and cortical structures involved with both movement and cognition, including primary motor cortex (6,8,32) and frontoparietal regions (6,7,9,33). In addition, the association between disease of white matter connections and mobility function is well documented (10). In the context of this literature, our findings support the idea from white matter lesion work that brain connectivity is altered with poor mobility function, while highlighting a region of functional change that was not evident in volumetric studies.

One recent study has used a slightly different method, estimation of cortical thickness, to investigate relationships between the brain structure and gait (34). In this study, de Laat and colleagues observed that cortical thickness in the superior temporal gyrus has been associated with stride length and width. This finding is in accord with our observation and as well as earlier work suggesting that brain volume and cortical thickness capture different properties of grey matter (35).

This exploratory study is the first to demonstrate the importance of the organization of functional brain networks in understanding the relationship between the brain and mobility. Results should be interpreted keeping in mind the exploratory nature of the analyses, which limited the sample size and range of measures available. In addition, graph theory methods are currently an active area of study, as noted in the Methods section. It is important to replicate these results in a larger, better characterized cohort and for the methods to be applied in other data sets. However, these findings open up intriguing avenues for future studies, including the importance of the interplay between sensory function, the brain, and mobility, and the insights that can be provided by applying new cutting-edge analysis methods, particularly graph theory.

Supplementary Material

Supplementary material can be found at: http://biomedgerontology.oxfordjournals.org/

Funding

This work was supported by the Clinical Research Unit at Wake Forest School of Medicine (M01-RR07122), the Translational Science Center at Wake Forest University, and the Wake Forest Claude D. Pepper Older Americans Independence Center (P30 AG21332). C.H. was supported in part by a grant through the American Federation for Aging Research (RAG12516). Data collection by John Tobben and Sean Miller was supported by the National Institutes of Health/National Institute of Diabetes and Digestive and Kidney Disease (T35 DK007400-32).

Acknowledgments

The authors would also like to thank Crystal Blair, Debra Hege, John Tobben, Sean Miller, and the staff at the Center for Biomolecular Imaging at Wake Forest School of Medicine for their efforts collecting data.

References

1. Rosso AL, Studenski SA, Chen WG, et al. Aging, the central nervous system, and mobility. *J Gerontol A Biol Sci Med Sci*. 2013;68:1379–1386. doi:10.1093/gerona/glt089
2. Inzitari M, Newman AB, Yaffe K, et al. Gait speed predicts decline in attention and psychomotor speed in older adults: the health aging and body composition study. *Neuroepidemiology*. 2007;29:156–162. doi:10.1159/000111577
3. Atkinson HH, Rosano C, Simonsick EM, et al.; Health ABC study. Cognitive function, gait speed decline, and comorbidities: the health, aging and body composition study. *J Gerontol A Biol Sci Med Sci*. 2007;62:844–850.
4. Holtzer R, Verghese J, Xue X, Lipton RB. Cognitive processes related to gait velocity: results from the Einstein Aging Study. *Neuropsychology*. 2006;20:215–223. doi:10.1037/0894-4105.20.2.215
5. Nadkarni NK, Nunley KA, Aizenstein H, et al.; for the Health ABCS. Association between cerebellar gray matter volumes, gait speed, and information-processing ability in older adults enrolled in the Health ABC study. *J Gerontol A Biol Sci Med Sci*. October 29, 2013. doi:10.1093/gerona/glt151
6. Rosano C, Aizenstein H, Brach J, Longenberger A, Studenski S, Newman AB. Special article: gait measures indicate underlying focal gray matter atrophy in the brain of older adults. *J Gerontol A Biol Sci Med Sci*. 2008;63:1380–1388.
7. Rosano C, Aizenstein HJ, Studenski S, Newman AB. A regions-of-interest volumetric analysis of mobility limitations in community-dwelling older adults. *J Gerontol A Biol Sci Med Sci*. 2007;62:1048–1055.

8. Rosano C, Bennett DA, Newman AB, et al. Patterns of focal gray matter atrophy are associated with bradykinesia and gait disturbances in older adults. *J Gerontol A Biol Sci Med Sci*. 2012;67:957–962. doi:10.1093/gerona/glr262
9. Rosano C, Studenski SA, Aizenstein HJ, Boudreau RM, Longstreth WT Jr, Newman AB. Slower gait, slower information processing and smaller prefrontal area in older adults. *Age Ageing*. 2012;41:58–64. doi:10.1093/ageing/afr113
10. Zheng JJ, Delbaere K, Close JC, Sachdev PS, Lord SR. Impact of white matter lesions on physical functioning and fall risk in older people: a systematic review. *Stroke*. 2011;42:2086–2090. doi:10.1161/STROKEAHA.110.610360
11. Laurienti PJ, Joyce KE, Telesford QK, Burdette JH, Hayasaka S. Universal fractal scaling of self-organized networks. *Physica A*. 2011;390:3608–3613. doi:10.1016/j.physa.2011.05.011
12. Guralnik JM, Simonsick EM, Ferrucci L, et al. A short physical performance battery assessing lower extremity function: association with self-reported disability and prediction of mortality and nursing home admission. *J Gerontol*. 1994;49:M85–M94.
13. Bravo G, Hébert R. Age- and education-specific reference values for the Mini-Mental and modified Mini-Mental State Examinations derived from a non-demented elderly population. *Int J Geriatr Psychiatry*. 1997;12:1008–1018.
14. Bohn MJ, Babor TF, Kranzler HR. The Alcohol Use Disorders Identification Test (AUDIT): validation of a screening instrument for use in medical settings. *J Stud Alcohol*. 1995;56:423–432.
15. Selzer ML. The Michigan alcoholism screening test: the quest for a new diagnostic instrument. *Am J Psychiatry*. 1971;127:1653–1658.
16. Haringsma R, Engels GI, Beekman AT, Spinhoven P. The criterion validity of the Center for Epidemiological Studies Depression Scale (CES-D) in a sample of self-referred elders with depressive symptomatology. *Int J Geriatr Psychiatry*. 2004;19:558–563. doi:10.1002/gps.1130
17. Guralnik JM, Ferrucci L, Pieper CF, et al. Lower extremity function and subsequent disability: consistency across studies, predictive models, and value of gait speed alone compared with the short physical performance battery. *J Gerontol A Biol Sci Med Sci*. 2000;55:M221–M231.
18. Hutchison RM, Womelsdorf T, Allen EA, et al. Dynamic functional connectivity: promise, issues, and interpretations. *Neuroimage*. 2013;80:360–378. doi:10.1016/j.neuroimage.2013.05.079
19. Whitlow CT, Casanova R, Maldjian JA. Effect of resting-state functional MR imaging duration on stability of graph theory metrics of brain network connectivity. *Radiology*. 2011;259:516–524. doi:10.1148/radiol.11101708
20. Newman ME. Modularity and community structure in networks. *Proc Natl Acad Sci U S A*. 2006;103:8577–8582. doi:10.1073/pnas.0601602103
21. Newman ME, Girvan M. Finding and evaluating community structure in networks. *Phys Rev E Stat Nonlin Soft Matter Phys*. 2004;69(2 Pt 2):026113.
22. Steen M, Hayasaka S, Joyce K, Laurienti P. Assessing the consistency of community structure in complex networks. *Phys Rev E Stat Nonlin Soft Matter Phys*. 2011;84(1 Pt 2):016111.
23. Moussa MN, Steen MR, Laurienti PJ, Hayasaka S. Consistency of network modules in resting-state FMRI connectome data. *PLoS One*. 2012;7:e44428. doi:10.1371/journal.pone.0044428
24. Maldjian JA, Laurienti PJ, Kraft RA, Burdette JH. An automated method for neuroanatomic and cytoarchitectonic atlas-based interrogation of fMRI data sets. *Neuroimage*. 2003;19:1233–1239. doi:S1053811903001691 [pii]
25. Karim H, Fuhrman SI, Sparto P, Furman J, Huppert T. Functional brain imaging of multi-sensory vestibular processing during computerized dynamic posturography using near-infrared spectroscopy. *Neuroimage*. 2013;74:318–325. doi:10.1016/j.neuroimage.2013.02.010
26. Augustine JR. Circuitry and functional aspects of the insular lobe in primates including humans. *Brain Res Brain Res Rev*. 1996;22:229–244.
27. Lopez C, Blanke O, Mast FW. The human vestibular cortex revealed by coordinate-based activation likelihood estimation meta-analysis. *Neuroscience*. 2012;212:159–179. doi:10.1016/j.neuroscience.2012.03.028
28. Uddin LQ, Kinnison J, Pessoa L, Anderson ML. Beyond the tripartite cognition-emotion-interoception model of the human insular cortex. *J Cogn Neurosci*. 2014;26:16–27. doi:10.1162/jocn_a_00462
29. Lopez C, Blanke O. The thalamocortical vestibular system in animals and humans. *Brain Res Rev*. 2011;67:119–146. doi:10.1016/j.brainresrev.2010.12.002
30. Seltzer B, Pandya DN. Afferent cortical connections and architectonics of the superior temporal sulcus and surrounding cortex in the rhesus monkey. *Brain Res*. 1978;149:1–24.
31. Jürgens U. The efferent and afferent connections of the supplementary motor area. *Brain Res*. 1984;300:63–81.
32. Annweiler C, Beauchet O, Bartha R, et al. Motor cortex and gait in mild cognitive impairment: a magnetic resonance spectroscopy and volumetric imaging study. *Brain*. 2013;136(Pt 3):859–871. doi:10.1093/brain/aws373
33. Beauchet O, Annweiler C, Celle S, Bartha R, Barthelemy JC, Roche F. Higher gait variability is associated with decreased parietal gray matter volume among healthy older adults. *Brain Topogr*. May 17, 2013. doi:10.1007/s10548-013-0293-y.
34. de Laat KF, Reid AT, Grim DC, et al. Cortical thickness is associated with gait disturbances in cerebral small vessel disease. *Neuroimage*. 2012;59:1478–1484. doi:10.1016/j.neuroimage.2011.08.005
35. Winkler AM, Kochunov P, Blangero J, et al. Cortical thickness or grey matter volume? The importance of selecting the phenotype for imaging genetics studies. *Neuroimage*. 2010;53:1135–1146. doi:10.1016/j.neuroimage.2009.12.028